BCS-BEC crossover induced by a synthetic non-Abelian gauge field

Jayantha P. Vyasanakere, Shizhong Zhang, and Vijay B. Shenoy

Phys. Rev. B **84**, 014512 — Published 25 July 2011

DOI: 10.1103/PhysRevB.84.014512

BCS-BEC crossover induced by a synthetic non-Abelian gauge field

Jayantha P. Vyasanakere[1],* Shizhong Zhang[2],† and Vijay B. Shenoy[1‡]
[1] *Centre for Condensed Matter Theory, Department of Physics, Indian Institute of Science, Bangalore 560 012, India and*
[2] *Department of Physics, Ohio State University, Columbus, OH 43210*

We investigate the ground state of interacting spin-$\frac{1}{2}$ fermions in 3D at a finite density ($\rho \sim k_F^3$) in the presence of a uniform non-Abelian gauge field. The gauge field configuration (GFC) described by a vector $\boldsymbol{\lambda} \equiv (\lambda_x, \lambda_y, \lambda_z)$, whose magnitude λ determines the gauge coupling strength, generates a generalized Rashba spin-orbit interaction. For a weak attractive interaction in the singlet channel described by a small negative scattering length ($k_F|a_s| \lesssim 1$), the ground state in the absence of the gauge field ($\lambda = 0$) is a BCS (Bardeen-Cooper-Schrieffer) superfluid with large overlapping pairs. With increasing gauge-coupling strength, a non-Abelian gauge field engenders a crossover of this BCS ground state to a BEC (Bose-Einstein condensate) of bosons even with a weak attractive interaction that fails to produce a two-body bound state in free vacuum ($\lambda = 0$). For large gauge couplings ($\lambda/k_F \gg 1$), the BEC attained is a condensate of bosons whose properties are *solely* determined by the Rashba gauge field (and not by the scattering length so long as it is non-zero) – we call these bosons "rashbons". In the absence of interactions ($a_s = 0^-$), the shape of the Fermi surface of the system undergoes a topological transition at a critical gauge coupling λ_T. For high-symmetry GFCs we show that the crossover from the BCS superfluid to the rashbon BEC occurs in the regime of λ near λ_T. In the context of cold atomic systems, these results make an interesting suggestion of obtaining BCS-BEC crossover through a route other than tuning the interaction between the fermions.

PACS numbers: 03.75.Ss, 05.30.Fk, 67.85.-d, 67.85.Lm, 71.70.Ej

I. INTRODUCTION

Recent experimental progress in the generation of synthetic gauge fields[1–3] has enhanced the possibilities of controlled experimental studies of outstanding problems of quantum condensed matter and even of high energy physics[4] using cold atomic systems. Many theoretical works[5–8] have explored the possibilities of generating and physical origins of both Abelian and non-Abeilan gauge fields. The experimental work with synthetic gauge fields has been with bosonic ^{87}Rb atoms. In a recent commentary[9] , the investigation of fermions in synthetic non-Abelian gauge fields has been identified as a key research direction.

The study of interacting fermions in 3D space with controlled interactions has been one of the key successes of cold atoms research.[10–12] A particular example is the problem of the crossover from a BCS ground state with large overlapping pairs to a BEC of tightly bound bosonic pairs with increasing strength of attractive interactions – a phenomenon that was suggested many years earlier.[13–15] The superfluid transition temperature on the BCS side is determined by the superfluid energy gap, while on the BEC side it is determined by the condensation temperature of the tightly bound bosonic pairs of fermions.[16] A review of BCS-BEC crossover that is particularly useful in the context of this paper may be found in reference [17].

An interesting question is regarding the fate of interacting fermions in the presence of a non-Abelian gauge field. Motivated by the fact that even a spatially uniform non-Abelian gauge field produces interesting physical effects for bosons,[3,18,19] we focus on interacting fermions in uniform non-Abelian gauge fields.

In a recent paper,[20] two of us investigated how a uniform non-Abelian gauge field influences the bound state of two spin-$\frac{1}{2}$ fermions interacting via a contact attraction in the singlet channel characterized by a s-wave scattering length a_s. The type of uniform non-Abelian gauge field considered in that work leads to a generalized Rashba spin-orbit interaction. A key finding of that work is that for high-symmetry GFCs (more precisely defined in the next section), a two-body bound state exists for *any* scattering length however small and negative. The study suggested that the BCS-BEC crossover is drastically affected by a non-Abelian gauge field.

Here, motivated by the results of reference [20], we study *the many-body ground state of a finite density of interacting fermions in a non-Abelian gauge field by means of mean field theory.* At a fixed interaction (fixed scattering length a_s) however small and negative, we show that increasing the strength of a non-Abelian gauge field produces a crossover from a BCS superfluid (which is the ground state in the absence of the gauge field) to a BEC of bosons. Further, the bosons that condense to form the BEC at large gauge couplings are tightly bound pairs of fermions whose properties are determined *solely* by the non-Abelian gauge field – we have ventured to call these bosons "rashbons". For a given attractive interaction (fixed a_s), therefore, the crossover takes the standard BCS superfluid state to a rashbon BEC. There is an additional feature of the crossover that is particularly noteworthy. The Fermi surface of the non-interacting system ($a_s = 0^-$) undergoes a transition in its topology with increasing gauge-coupling strength. We show that for high-symmetry GFCs, the crossover regime of gauge couplings in the presence of interactions overlaps with the regime of topological transition of the non-interacting Fermi surface. In a sense this provides a "geometrical" view of the crossover.

The background and the statement of the problem we address along with a summary of our results are given in Section II. The mean field formulation is detailed in Section III. Section IV describes the results in detail. The paper is concluded with a discussion in Section V. We recommend the reading of Section II and Section V to obtain a physical picture of our results.

II. QUESTION ADDRESSED AND SUMMARY OF RESULTS

In units where the mass of the fermions and Planck's constant are set to unity, the hamiltonian of the fermions moving in a uniform non-Abelian gauge field is

$$\mathcal{H}_{GF} = \int \mathrm{d}^3\boldsymbol{r}\, \Psi^\dagger(\boldsymbol{r}) \left[\frac{1}{2}(\boldsymbol{p}\mathbf{1} - \boldsymbol{A}^\mu\tau^\mu)\cdot(\boldsymbol{p}\mathbf{1} - \boldsymbol{A}^\mu\tau^\mu)\right]\Psi(\boldsymbol{r}), \tag{1}$$

where $\Psi(\boldsymbol{r}) = \{\psi_\sigma(\boldsymbol{r})\}, \sigma = \uparrow, \downarrow$ are fermion operators, $\boldsymbol{p}$ is the momentum, $\boldsymbol{A}^\mu \equiv A_i^\mu \boldsymbol{e}_i$, are uniform gauge fields, τ^μ ($\mu = x, y, z$, generator index) are Pauli matrices and $\boldsymbol{e}_i$'s are the unit vectors in the i-th direction, $i = x, y, z$ (spatial index). As in [20], we specialize to $A_i^\mu = \lambda_i \delta_i^\mu$ leading to a hamiltonian with a generalized Rashba spin-orbit interaction

$$\mathcal{H}_R = \int \mathrm{d}^3\boldsymbol{r}\, \Psi^\dagger(\boldsymbol{r}) \left(\frac{\boldsymbol{p}^2}{2}\mathbf{1} - \boldsymbol{p}_\lambda\cdot\boldsymbol{\tau}\right)\Psi(\boldsymbol{r}), \tag{2}$$

where $\boldsymbol{p}_\lambda = \sum_i p_i\lambda_i\boldsymbol{e}_i$. The vector $\boldsymbol{\lambda} = \lambda\hat{\boldsymbol{\lambda}} = \sum_i \lambda_i\boldsymbol{e}_i$ describes a gauge field configuration (GFC) space as depicted in fig. 1; we call $\lambda = |\boldsymbol{\lambda}|$ as the gauge-coupling strength. GFCs have been classified in [20] as prolate, spherical, oblate

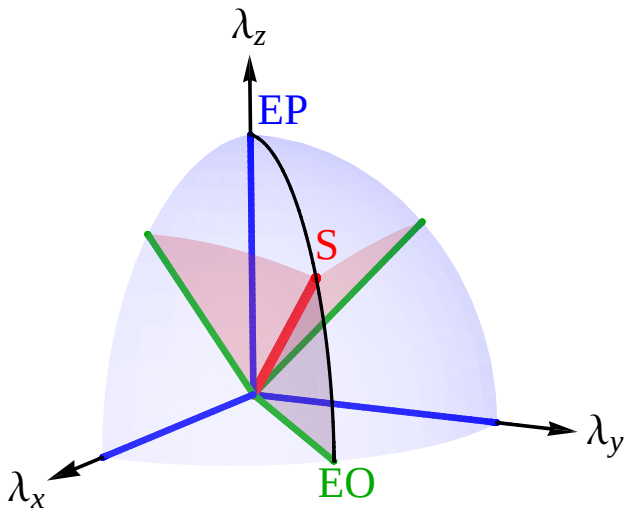

FIG. 1. (Color online) Gauge field configuration (GFC) space. The non-Abelian gauge field of eqn. (2) is described by a vector $\boldsymbol{\lambda} = (\lambda_x, \lambda_y, \lambda_z) = \lambda\hat{\boldsymbol{\lambda}}$, where $\lambda = |\boldsymbol{\lambda}|$ is the gauge-coupling strength and $\hat{\boldsymbol{\lambda}}$ is a unit vector. High-symmetry GFCs such as extreme prolate (EP, $\hat{\boldsymbol{\lambda}} = (0, 0, 1)$), spherical (S, $\hat{\boldsymbol{\lambda}} = \frac{1}{\sqrt{3}}(1, 1, 1)$) and extreme oblate (EO, $\hat{\boldsymbol{\lambda}} = \frac{1}{\sqrt{2}}(1, 1, 0)$) are as shown.

and generic. Of particular interest are the high-symmetry configurations shown in fig. 1 called extreme prolate (EP), spherical (S) and extreme oblate (EO).

The one-particle states of $\mathcal{H}_R$ are

$$|\boldsymbol{k}\alpha\rangle = |\boldsymbol{k}\rangle \otimes |\alpha\hat{\boldsymbol{k}}_\lambda\rangle \tag{3}$$

that disperse as

$$\varepsilon_{\boldsymbol{k}\alpha} = \frac{k^2}{2} - \alpha|\boldsymbol{k}_\lambda| \tag{4}$$

where $\boldsymbol{k}$-the momentum, and $\alpha = \pm 1$-the eigenvalues of the helicity operator $\hat{\boldsymbol{p}}_\lambda \cdot \boldsymbol{\tau}$, are the good quantum numbers. The quantity $\boldsymbol{k}_\lambda$ is defined analogously with $\boldsymbol{p}_\lambda$ in eqn. (2).

The interaction between the fermions is described by a contact attraction in the singlet channel

$$\mathcal{H}_\upsilon = \upsilon \int \mathrm{d}^3\boldsymbol{r}\, \psi^\dagger_\uparrow(\boldsymbol{r})\psi^\dagger_\downarrow(\boldsymbol{r})\psi_\downarrow(\boldsymbol{r})\psi_\uparrow(\boldsymbol{r}). \tag{5}$$

The endemic ultraviolet divergence of the theory described by the hamiltonian

$$\mathcal{H} = \mathcal{H}_R + \mathcal{H}_\upsilon \tag{6}$$

is handled[21] by introducing an ultraviolet momentum cutoff Λ. This entails characterization of the attraction by a physical parameter that describes the low energy scattering properties while making the parameter υ depend on Λ. More precisely,

$$\frac{1}{\upsilon} + \Lambda = \frac{1}{4\pi a_s} \tag{7}$$

where a_s is the s-wave scattering length in free vacuum, i. e., when the gauge field is absent ($\lambda = 0$). In free vacuum (3D) only an attraction larger than a critical strength can produce a two-particle bound state. This is embodied in the fact that for $a_s < 0$ (BCS side) there is no two-body bound state; a bound state develops only as $a_s \to -\infty$, or $\frac{1}{a_s} \to 0^-$ (resonance). For $a_s > 0$ (BEC side) a bound state is obtained with a binding energy $E_b = \frac{1}{a_s^2}$.

GFC	a_{sc}	$a_s<0$ $\lambda\lvert a_s\rvert \ll 1$			Resonance $1/(\lambda a_s)=0$			$a_s>0$ $\lambda a_s \ll 1$		
		E_b	η_t	Spin Structure	E_b	η_t	Spin Structure	E_b	η_t	Spin Structure
EP	$-\infty$	No bound state			0	$\frac{1}{2}$	Bi-axial nematic (BW)	$\frac{1}{a_s^2}$	0	singlet
S	0^-	$\frac{\lambda^4 a_s^2}{3}$	$\frac{1}{2}$	Spherical	$\frac{\lambda^2}{3}$	$\frac{1}{4}$	Spherical	$\frac{1}{a_s^2}+\frac{2\lambda^2}{3}$	0	singlet
EO	0^-	$\frac{2\lambda^2}{e^2}e^{-\frac{2\sqrt{2}}{\lambda\lvert a_s\rvert}}$	$\frac{1}{2}$	Uni-axial nematic (ABM)	$0.22\lambda^2$	0.28	Uni-axial nematic (ABM)	$\frac{1}{a_s^2}+\frac{\lambda^2}{2}$	0	singlet

TABLE I. Summary of the two-body problem[20] in high-symmetry GFCs ($\lambda > 0$). E_b is the binding energy and η_t is the triplet content (not reported in reference [20]). The bi-axial spin nematic structure is similar to the BW (Balian-Werthamer) or B-phase[15] of ^{3}He, and the uni-axial spin nematic structure to that of the ABM (Anderson-Brinkman-Morel) or A-phase[15] of ^{3}He. The values of E_b and η_t at resonance, which correspond to the properties of the rashbon (for S and EO cases), are exact results, while others are asymptotic values in the regimes indicated.

A. Summary of the two-body problem[20]

A uniform non-Abelian gauge field brings about remarkable changes in the two-body problem as shown in reference [20]. Most vividly, for high-symmetry GFCs such as S and EO, the critical scattering length a_{sc} required for the formation of a bound state vanishes, i. e., there is a two body bound state for *any* scattering length however small and negative (deep BCS side). The size of the binding energy of the bound state depends on the GFC. On the BCS side, the binding energy has an exponential dependence on a_s and λ for the EO GFC while for the S GFC this dependence is algebraic. Another interesting aspect that emerges is the symmetry of the bound-state wave function. In a non-Abelian gauge field, the normalized bound-state wave function is made up of spatially symmetric singlet and spatially antisymmetric triplet pieces

$$|\psi_b\rangle = |\psi_s\rangle + |\psi_t\rangle. \tag{8}$$

Time reversal symmetry of the hamiltonian is preserved and this two-body-bound-state wave function picks up a nematic spin structure consistent with the symmetry of the GFC. The quadrupole operator is defined as $Q^{\alpha\beta} = \frac{1}{2}\left(\mathcal{S}^\alpha\mathcal{S}^\beta + \mathcal{S}^\beta\mathcal{S}^\alpha\right) - \frac{\langle\mathcal{S}^2\rangle}{3}\delta^{\alpha\beta}$ where $\mathcal{S}^\alpha$ are spin operators. A nematic state has $\langle\mathcal{S}^\alpha\rangle = 0$, while $\langle Q^{\alpha\beta}\rangle \neq 0$. In the present context, the singlet piece of the two-body wave function does not contribute to the quadrupole moment, while the triplet wave function has $\langle\mathcal{S}^\alpha\rangle = 0$, but $\langle Q^{\alpha\beta}\rangle \neq 0$. The triplet content of the wave function is characterized by a parameter

$$\eta_t = \langle\psi_t|\psi_t\rangle. \tag{9}$$

which, therefore, is also a measure of the nematicity.

The binding energy E_b, the triplet content η_t and the spin symmetry of the two-body wave function for different GFCs are summarized[22] in Table I. The gist of reference [20] is that high-symmetry GFCs induce high degeneracy that enhances the low-energy (infrared) density of states and this promotes bound state formation. Colloquially, high-symmetry GFCs are "attractive interaction amplifiers". An aspect that is important in the discussion below is that the physics of the two-body problem in the presence of the gauge field ($\lambda > 0$) is completely determined by the dimensionless parameter λa_s. All aspects of the solution depends only on λa_s when length and energy are respectively measured in units of λ^{-1} and λ^2. This is true for any GFC (*except EP GFC*) as is evident from Table. I The EP GFC is an exception because the *kinetic energy content inside the non-interacting Fermi sea is unaltered by the increase*

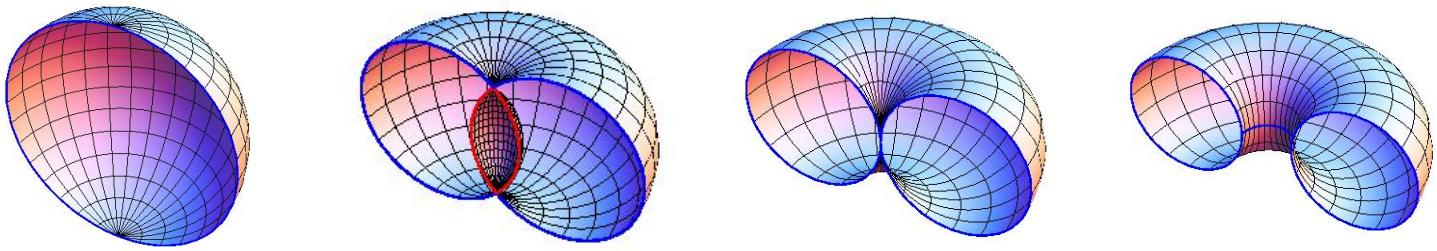

(a) $\lambda = 0$ **(b)** $0 < \lambda < \lambda_T$ **(c)** $\lambda = \lambda_T$ **(d)** $\lambda > \lambda_T$

FIG. 2. (Color online) Fermi surface topology transition (FSTT) with increasing gauge-coupling strength for EO GFC. **(a)** Two overlapping spherical Fermi surfaces in the absence of a gauge field **(b)** A gauge coupling smaller than λ_T: The union of the + and − Fermi surfaces forms a spindle torus. The apple of the spindle torus is the + helicity Fermi surface which is shown with a blue border, and the lemon of the spindle torus is the − helicity Fermi surface which is shown with a red border. **(c)** The gauge coupling that obtains the FSTT. The + helicity Fermi surface is a horn torus, while the − helicity Fermi surface vanishes. **(d)** For a gauge coupling larger than λ_T, there is only the + helicity Fermi surface which is a ring torus. Note that all the figures show only a sectioned half of the Fermi surfaces.

of λ. Therefore, the gauge coupling λ stays neutral in the competition between kinetic energy and the attractive interaction. This is the reason why the energetics of the two-body problem is unaffected by the presence of an EP gauge field (see Table. I).

B. Synopsis of the new results of this paper: Evolution of the many-body ground state with gauge coupling

In this paper we investigate the system described by the hamiltonian of eqn. (6) at a *finite density* ρ of the fermions. The finite density introduces an additional energy scale which can be conveniently taken to be the Fermi energy E_F (and an associated Fermi wave vector k_F) in the *absence* of the gauge field ($\lambda = 0$)

$$E_F = \frac{k_F^2}{2} = \frac{1}{2}(3\pi^2\rho)^{2/3}. \tag{10}$$

At finite densities of fermions, therefore, the ground state of the system (zero temperature) is determined by the dimensionless parameters $k_F a_s$, λ/k_F, and the direction $\hat{\boldsymbol{\lambda}}$ in GFC space. We work at fixed density and $k_F a_s$, and study the evolution of the ground state with λ/k_F for different $\hat{\boldsymbol{\lambda}}$s corresponding to high-symmetry GFCs.

The possibility of interesting physics in this system is suggested by the following observation which provided one of the motivations for this work. Consider a system of *non-interacting* (NI) fermions ($\mathcal{H}_v = 0$ in eqn. (6)). In the absence of a gauge field ($\lambda = 0$), the ground state has a chemical potential E_F and is described by two identical filled Fermi seas bounded by spherical Fermi surfaces of radius k_F – one each for $\uparrow$ and $\downarrow$ spins. In the presence of the gauge field ($\lambda \neq 0$), the helicity α is the good quantum number along with momentum (see eqn. (3)), and hence the ground state will be two Fermi seas, one for each helicity. The chemical potential[23] now depends on λ through a function $\mu_{NI}(\lambda)$ that is determined by $\hat{\boldsymbol{\lambda}}$. Both of the Fermi seas are generically non-spherical with a shape determined by $\hat{\boldsymbol{\lambda}}$. Since the one-particle states with same momentum but with opposite helicities are non-degenerate (see eqn. (4)), the Fermi surfaces of different helicities are not identical and evolve differently with increasing λ (at a fixed density ρ). The most interesting aspect is that since the + helicity state is lower in energy than the − helicity one for all momenta, upon increasing λ, the volume enclosed by the + helicity Fermi surface increases at the expense of that of the − helicity Fermi surface. Matters come to a head at a critical gauge coupling λ_T (which depends on $\hat{\boldsymbol{\lambda}}$) where the − helicity Fermi sea ceases to exist since the chemical potential $\mu_{NI}(\lambda)$ falls below the bottom of the − helicity band. Thus, for $\lambda \geq \lambda_T$ the ground state is a Fermi sea of only + helicity. This is illustrated for the EO GFC in fig. 2. The values of λ_T determined by the density of particles for different high-symmetry GFCs are given in Table II; it is to be noted that in all cases λ_T is of order k_F. Another aspect to be noted is that there is a *change in the topology* of the + helicity Fermi surface at λ_T. We call this the "Fermi surface topology transition" (FSTT) – hence the subscript T in λ_T. For example, in the EO case, the genus of the + helicity Fermi surface changes from zero (homeomorphic to a sphere) to unity (homeomorphic to a torus) at λ_T as illustrated in fig. 2. We emphasize here that our use of the

GFC	λ_T	$\lambda \ll \lambda_T$ Before FSTT			$\lambda \gg \lambda_T$ After FSTT			Crossover to rashbon-BEC
		μ	η_t	Spin Structure	μ	η_t	Spin Structure	as $\lambda \to \infty$?
EP	k_F	$\approx E_F$	$\propto \lambda^2$	Bi-axial nematic	$\approx E_F$	$\frac{1}{2}$	Bi-axial nematic	No
S	$\frac{\sqrt{3}}{2^{(2/3)}} k_F$	$\approx \mu_{NI}(\lambda)$ (eqn. (34))	$\propto \lambda^2$	Spherical	$\approx -\frac{\lambda^2}{6}$	$\approx \frac{1}{4}$	Spherical	Yes
EO	$\left(\frac{8\sqrt{2}}{3\pi}\right)^{\frac{1}{3}} k_F$	$\approx \mu_{NI}(\lambda)$ (eqn. (37))	$\propto \lambda^2$	Uni-axial nematic	$\approx -0.11\lambda^2$	≈ 0.28	Uni-axial nematic	Yes

TABLE II. Summary of the properties of the superfluid ground state for two regimes of the gauge-coupling strength λ. The results shown here are for a weak attractive interaction ($a_s < 0, k_F|a_s| \ll 1$). μ is the ground state chemical potential and η_t is the triplet content of the pair wave function. Well before the FSTT ($\lambda \ll \lambda_T$), the ground state is a BCS superfluid. In the regime ($\lambda \gg \lambda_T$), for the S and EO GFCs, the chemical potential is close to half of the rashbon energy (see Table. I) and the pair wave function attains the same triplet content as that of the rashbon, clearly indicating a crossover from a BCS superfluid to a rashbon condensate. Any GFC *except* EP produces a BCS - rashbon BEC crossover.

phrase "transition" is *not* to suggest that an order parameter emerges from any broken symmetry for $\lambda > \lambda_T$, rather it connotes a change in the topology of the Fermi surface and the concomitant low energy excitations. For $\lambda < \lambda_T$, there are low energy excitations of both helicities, while for $\lambda > \lambda_T$ low energy excitations are only of the + helicity.

What happens in the *presence* of interactions ($\mathcal{H}_v \neq 0$ in eqn. (5))? Consider an interaction with a small negative scattering length ($k_F|a_s| \ll 0$, deep BCS side). For $\lambda \ll \lambda_T$, the ground state is a superfluid with large overlapping pairs and an exponentially small excitation gap. The chemical potential of this state is nearly unaffected and is $\mu_{NI}(\lambda)$, that of the non-interacting system in a gauge field. The only qualitative difference from the usual s-wave BCS state is that the pair wave function now has a small triplet content and an associated spin nematicity induced by the gauge field. This picture changes drastically in the case of high-symmetry GFCs (such as S and EO) when the gauge-coupling strength λ is tuned past λ_T. The key new finding of this paper is that *for high-symmetry GFCs, a BEC of tightly bound pairs is obtained for $\lambda \gg \lambda_T$ even with a small negative scattering length.* In other words, one can engineer a BCS-BEC crossover with a high-symmetry GFC by increasing the gauge-coupling strength even with a very weak attractive interaction that is unable to produce a two-body bound state in free vacuum. This result arises from the fact that for $\lambda \gg \lambda_T$, the size of the *two-body* bound-state wave function (see Table I) becomes smaller than the inter-particle spacing. The fermions therefore form tightly bound pairs which then Bose condense in the zero center of mass momentum state. As is evident from the discussion, the physics of these results owes to the character of high-symmetry GFCs to act as attractive interaction amplifiers. Indeed, as $\lambda/\lambda_T \to \infty$ the chemical potential tends to that determined by the two-particle bound-state energy. Since $\lambda|a_s| \to \infty$ (fixed a_s), the nature of the *two body bound state obtained is identical to that obtained with a resonant scattering length in the presence of the gauge field* as tabulated in Table I. The properties of this bosonic bound state of two fermions is *determined solely by the Rashba gauge field*; we call these emergent bosons as "rashbons" (see Section IV B and second paragraph of Section V for details). The BEC that is obtained for $\lambda \gg \lambda_T$ is a rashbon condensate. The results for various GFCs are tabulated in Table II which is a summary of this paper.

In the remaining sections we illustrate these conclusions by a mean field theory of the superfluid ground state of this interacting fermion system. Mean field theory is known to give a qualitatively correct description for the superfluid ground state.[24]

III. MEAN FIELD THEORY

We now describe the details of the mean field analysis of the superfluid ground state of fermions in a non-Abelian gauge field. This analysis involves certain straightforward manipulations beyond the standard formulation,[17] and hence presented in detail. The present analysis can treat *any* GFC. Results for specific GFCs of interest will be presented in the next section.

To perform a mean-field analysis of the superfluid ground state we recast the interaction term $\mathcal{H}_v$ in a convenient

form

$$\mathcal{H}_\upsilon = \frac{\upsilon}{2}\int \mathrm{d}^3\boldsymbol{r}\, S^\dagger(\boldsymbol{r})S(\boldsymbol{r}), \tag{11}$$

where $S^\dagger(\boldsymbol{r})$ is the singlet creation operator

$$S^\dagger(\boldsymbol{r}) = \frac{1}{\sqrt{2}}\left(\psi^\dagger_\uparrow(\boldsymbol{r})\psi^\dagger_\downarrow(\boldsymbol{r}) - \psi^\dagger_\downarrow(\boldsymbol{r})\psi^\dagger_\uparrow(\boldsymbol{r})\right). \tag{12}$$

The interaction in terms of the singlet operators can be cast in momentum space

$$\mathcal{H}_\upsilon = \frac{\upsilon}{2V}\sum_{\boldsymbol{q}} S^\dagger(\boldsymbol{q})S(\boldsymbol{q}), \tag{13}$$

where V is the volume of the system and the mean-field ansatz corresponds to taking

$$\langle S(\boldsymbol{q})\rangle = \langle S\rangle\delta_{\boldsymbol{q},\boldsymbol{0}}, \tag{14}$$

where $\langle S\rangle = \langle S(\boldsymbol{0})\rangle$ with

$$S^\dagger(\boldsymbol{0}) = \frac{1}{\sqrt{2}}\sum_{\boldsymbol{k}}\left(c^\dagger_{\boldsymbol{k}\uparrow}c^\dagger_{-\boldsymbol{k}\downarrow} - c^\dagger_{\boldsymbol{k}\downarrow}c^\dagger_{-\boldsymbol{k}\uparrow}\right). \tag{15}$$

The fermion operators $c^\dagger_{\boldsymbol{k}\sigma}$ are defined by

$$c^\dagger_{\boldsymbol{k}\sigma} = \frac{1}{\sqrt{V}}\int \mathrm{d}^3\boldsymbol{r}\, e^{-i\boldsymbol{k}\cdot\boldsymbol{r}}\psi^\dagger_\sigma(\boldsymbol{r}). \tag{16}$$

It is now convenient to sum *only over half* of the allowed $\boldsymbol{k}$ values in eqn. (15)

$$S(\boldsymbol{0}) = \sqrt{2}\sum_{\boldsymbol{k}}{}' \left(c^\dagger_{\boldsymbol{k}\uparrow}c^\dagger_{-\boldsymbol{k}\downarrow} - c^\dagger_{\boldsymbol{k}\downarrow}c^\dagger_{-\boldsymbol{k}\uparrow}\right) \tag{17}$$

as is here and henceforth indicated by the prime over the summation symbol. The advantage of this exercise is that the operator $S(\boldsymbol{0})$ can be written in the helicity basis as

$$S(\boldsymbol{0}) = \sqrt{2}\sum_{\boldsymbol{k}\alpha}{}' \alpha c^\dagger_{\boldsymbol{k}\alpha}c^\dagger_{-\boldsymbol{k}\alpha} \tag{18}$$

Introducing a chemical potential μ, we obtain the mean-field Hamiltonian as

$$\begin{aligned}\mathcal{H}_{MF} = &\sum_{\boldsymbol{k}\alpha}\xi_{\boldsymbol{k}\alpha}c^\dagger_{\boldsymbol{k}\alpha}c_{\boldsymbol{k}\alpha} + \Delta\sum_{\boldsymbol{k}\alpha}{}' \alpha c^\dagger_{\boldsymbol{k}\alpha}c^\dagger_{-\boldsymbol{k}\alpha}\\ &+ \Delta\sum_{\boldsymbol{k}\alpha}{}' \alpha c_{-\boldsymbol{k}\alpha}c_{\boldsymbol{k}\alpha} - \frac{V\Delta^2}{\upsilon}\end{aligned} \tag{19}$$

where $c^\dagger_{\boldsymbol{k}\alpha}$ are electron operators associated with the one-particle helicity eigenstate (eqn. (3)), $\Delta = \frac{\upsilon\langle S\rangle}{\sqrt{2}V}$ is the order parameter (taken to be real), and $\xi_{\boldsymbol{k}\alpha} = \tilde{\varepsilon}_{\boldsymbol{k}\alpha} - \mu$. Here $\tilde{\varepsilon}_{\boldsymbol{k}\alpha}$ is $\varepsilon_{\boldsymbol{k}\alpha}$ referred to the bottom of the + helicity band. Noting inversion symmetry, $\xi_{-\boldsymbol{k}\alpha} = \xi_{\boldsymbol{k}\alpha}$, eqn. (19) can now be recast as

$$\begin{aligned}\mathcal{H}_{MF} = &\sum_{\boldsymbol{k}\alpha}{}' \begin{pmatrix} c^\dagger_{\boldsymbol{k}\alpha} & c_{-\boldsymbol{k}\alpha}\end{pmatrix}\begin{bmatrix}\xi_{\boldsymbol{k}\alpha} & \alpha\Delta\\ \alpha\Delta & -\xi_{\boldsymbol{k}\alpha}\end{bmatrix}\begin{pmatrix} c_{\boldsymbol{k}\alpha}\\ c^\dagger_{-\boldsymbol{k}\alpha}\end{pmatrix}\\ &+\sum_{\boldsymbol{k}\alpha}{}' \xi_{\boldsymbol{k}\alpha} - \frac{V\Delta^2}{\upsilon}\end{aligned} \tag{20}$$

which now has the standard form except for the fact that the summation over $\boldsymbol{k}$ is carried out only over half of the momentum space and a sum over the two helicities is taken.

The hamiltonian in eqn. (20) can now be diagonalized in terms of the Bogoliubov quasiparticle operators as

$$\begin{aligned}\mathcal{H}_{MF} &= \sum_{\boldsymbol{k}\alpha}{}' E_{\boldsymbol{k}\alpha}\left(\gamma^\dagger_{\boldsymbol{k}\alpha 1}\gamma_{\boldsymbol{k}\alpha 1} + \gamma^\dagger_{\boldsymbol{k}\alpha 2}\gamma_{\boldsymbol{k}\alpha 2}\right) \\ &+ \sum_{\boldsymbol{k}\alpha}{}' \left(\xi_{\boldsymbol{k}\alpha} - E_{\boldsymbol{k}\alpha}\right) - \frac{V\Delta^2}{\upsilon}\end{aligned} \tag{21}$$

where $E_{\boldsymbol{k}\alpha} = \sqrt{\xi^2_{\boldsymbol{k}\alpha} + \Delta^2}$ (Δ is also the excitation gap), and

$$\begin{aligned}\gamma_{\boldsymbol{k}\alpha 1} &= u_{\boldsymbol{k}\alpha} c_{\boldsymbol{k}\alpha} - \alpha v_{\boldsymbol{k}} c^\dagger_{-\boldsymbol{k}\alpha} \\ \gamma^\dagger_{\boldsymbol{k}\alpha 2} &= \alpha v_{\boldsymbol{k}\alpha} c_{\boldsymbol{k}\alpha} + u_{\boldsymbol{k}} c^\dagger_{-\boldsymbol{k}\alpha}\end{aligned} \tag{22}$$

with

$$u^2_{\boldsymbol{k}\alpha} = \frac{1}{2}\left(1 + \frac{\xi_{\boldsymbol{k}\alpha}}{E_{\boldsymbol{k}\alpha}}\right), \quad v^2_{\boldsymbol{k}\alpha} = \frac{1}{2}\left(1 - \frac{\xi_{\boldsymbol{k}\alpha}}{E_{\boldsymbol{k}\alpha}}\right). \tag{23}$$

A standard analysis now leads to the gap equation

$$-\frac{1}{\upsilon} = \frac{1}{V}\sum_{\boldsymbol{k}\alpha}{}' \frac{1}{2E_{\boldsymbol{k}\alpha}}. \tag{24}$$

Noting the inversion symmetry of the problem and using the renormalization of the interaction, the gap equation becomes

$$-\frac{1}{4\pi a_s} = \frac{1}{2V}\sum_{\boldsymbol{k}\alpha}\left(\frac{1}{2E_{\boldsymbol{k}\alpha}} - \frac{1}{k^2}\right). \tag{25}$$

The number equation is

$$\rho = \frac{1}{V}\sum_{\boldsymbol{k}\alpha}\frac{1}{2}\left(1 - \frac{\xi_{\boldsymbol{k}\alpha}}{E_{\boldsymbol{k}\alpha}}\right). \tag{26}$$

The solution of eqn. (25) along with the number equation (eqn. (26)), determines the chemical potential μ and the gap parameter Δ in the ground state.

The ground state $|\Psi_G\rangle$ of the system is given by

$$|\Psi_G\rangle = \prod_{\boldsymbol{k}\alpha}{}' (u_{\boldsymbol{k}\alpha} + \alpha v_{\boldsymbol{k}\alpha} c^\dagger_{\boldsymbol{k}\alpha} c^\dagger_{-\boldsymbol{k}\alpha})|0\rangle \tag{27}$$

where $|0\rangle$ is the fermion vacuum. This can be (up to a normalization) be re-written as

$$|\Psi_G\rangle = e^{P^\dagger}|0\rangle \tag{28}$$

where $P^\dagger$ is the pair creation operator given by

$$P^\dagger = \sum_{\boldsymbol{k}\alpha}{}' \alpha\phi_{\boldsymbol{k}\alpha} c^\dagger_{\boldsymbol{k}\alpha} c^\dagger_{-\boldsymbol{k}\alpha} \tag{29}$$

where $\phi_{\boldsymbol{k}\alpha} = \dfrac{v_{\boldsymbol{k}\alpha}}{u_{\boldsymbol{k}\alpha}}$. The singlet and triplet parts of the pair can be extracted by noting that

$$\begin{aligned}P^\dagger = &\underbrace{\sum_{\boldsymbol{k}}{}' \phi_s(\boldsymbol{k})\left(c^\dagger_{\boldsymbol{k}+} c^\dagger_{-\boldsymbol{k}+} - c^\dagger_{\boldsymbol{k}-} c^\dagger_{-\boldsymbol{k}-}\right)}_{\text{singlet}} \\ &+ \underbrace{\sum_{\boldsymbol{k}}{}' \phi_t(\boldsymbol{k})\left(c^\dagger_{\boldsymbol{k}+} c^\dagger_{-\boldsymbol{k}+} + c^\dagger_{\boldsymbol{k}-} c^\dagger_{-\boldsymbol{k}-}\right)}_{\text{triplet}}\end{aligned} \tag{30}$$

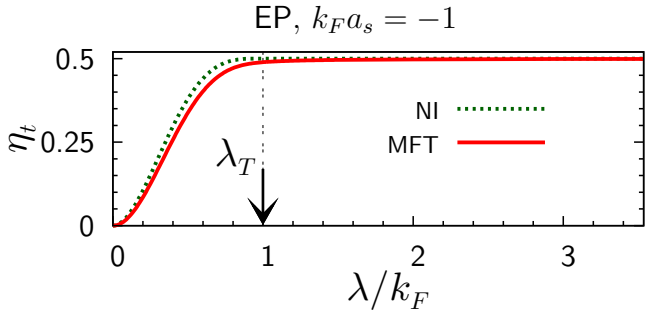

FIG. 3. (Color online) Evolution of the triplet content η_t of the pair wave function as a function of the gauge-coupling strength λ for an EP GFC with $k_F a_s = -1$. The evolution of the same quantity of the non interacting system ($a_s = 0^-$) is also shown for comparison.

with

$$\begin{aligned} \phi_s(\boldsymbol{k}) &= \frac{1}{2}\left(\phi_{\boldsymbol{k}+} + \phi_{\boldsymbol{k}-}\right) \\ \phi_t(\boldsymbol{k}) &= \frac{1}{2}\left(\phi_{\boldsymbol{k}+} - \phi_{\boldsymbol{k}-}\right). \end{aligned} \tag{31}$$

This analysis sheds light on how an attraction in the singlet channel in presence of a non-Abelian gauge field can produce a triplet piece in the pair wave function. The triplet content η_t is now defined as the weight of the triplet piece of the pair creation operator in eqn. (30). One can also charecterize this by an expectation value of the quadrupole operator of reference [22]. However, the definition for the triplet content η_t given above provides a physically transparent and a simple measure of the quantity of interest.

A remark about the Bogoliubov quasiparticles obtained in eqn. (22) is in order. It appears that for each helicity there are two branches of quasi-particle excitations labeled 1 and 2. Ostensibly, therefore, there are *four* branches of quasiparticles which at the first sight is surprising. Note, however, that these four branches are defined only in *half* of the momentum space. If the Bogoliubov excitations were defined for all $\boldsymbol{k}$, they will not be independent, for example, $\gamma^\dagger_{\boldsymbol{k}+2} \equiv \gamma^\dagger_{-\boldsymbol{k}+1}$. This is the motivation behind introduction of the sum over one half of the momentum space in eqn. (17). It is now clear that the formulation recovers the correct count of excitations, i.e., within the present formulation, two excitations for each $\boldsymbol{k}$ in momentum space is recovered as four excitations for each $\boldsymbol{k}$ in half the momentum space.

IV. RESULTS FOR SPECIFIC GAUGE FIELD CONFIGURATIONS

In this section, we shall present results of how the ground state of the system evolves with λ for different high-symmetry GFCs. We shall be concerned only with negative scattering lengths ($a_s < 0$) since this is the regime which has the most interesting physics. In the absence of the gauge field ($\lambda = 0$) there is no two-body bound state, and the usual BCS superfluid ground state[17] $|BCS_0\rangle$ is obtained. For small λ, i. e., $\lambda \ll \lambda_T$, we expect and find the ground state $|\Psi_G\rangle$ to be qualitatively close to $|BCS_0\rangle$ state with an exponentially small excitation gap and a chemical potential essentially unaltered from that of the non-interacting problem ($\mu_{NI}(\lambda)$). Except for the EP GFC, when λ is increased beyond λ_T, the chemical potential μ begins to fall and approaches $-E_b/2$, the value set by the energy of the two-body bound state. This signals the crossover to the BEC state. Additionally, the pair wave function defined by eqn. (29) approaches the wave function of the two-body bound state.

A summary of the results for various GFCs discussed below is given in Table. II.

A. Extreme prolate (EP) GFC

This GFC with $\boldsymbol{\lambda} = (0, 0, \lambda)$ has an FSTT at $\lambda_T = k_F$. Before FSTT ($\lambda < \lambda_T$), the + helicity Fermi sea consists of the volume enclosed by two intersecting spheres of radius k_F centered around $(0, 0, \pm\lambda)$, while the − helicity Fermi sea is the lens shaped region formed by the volume common to both spheres. When λ exceeds λ_T the − helicity Fermi surface vanishes, and the + helicity Fermi sea is made of two disjoint spheres centered at $(0, 0, \pm\lambda)$. The chemical potential $\mu_{NI}(\lambda) = E_F$, i. e., is unaffected by the EP gauge field.

For $k_F|a_s| \ll 1$, the standard result[17] for the excitation gap is

$$\frac{\Delta}{E_F} \approx \frac{8}{e^2} e^{-\frac{\pi}{2k_F|a_s|}} \tag{32}$$

and the chemical potential is

$$\mu \approx E_F. \tag{33}$$

Not unexpectedly, the excitation gap Δ and the chemical potential are *independent* of λ. The ground state for any λ is a superfluid state with large overlapping pairs, and *there is no BCS-BEC crossover* for the EP GFC. There is, however, a qualitative change in the spin structure of the pair wave function. With increasing λ, the pair wave function develops a triplet content η_t (see fig. 3) which attains a value close to $\frac{1}{2}$ at $\lambda = \lambda_T$ and stays so with further increase of λ. The physics behind this result can be traced to the speciality EP GFC discussed earlier.

It must be noted that the non-interacting ground state also has a triplet content (see Fig. 3). As is evident (see eqn. (30)), this arises from the fact that the + helicity Fermi sea is different (and larger) than the − helicity Fermi sea. The triplet content of the non-interacting system increases monotonically with λ and attains a value of $\frac{1}{2}$ at $\lambda = \lambda_T$ and remains at this value for any larger λ. As expected, in the presence of an attractive interaction in the singlet channel ($a_s < 0$), the pairs have a triplet content *less* than that of the non interacting system.

We note that the qualitative nature of the results for negative scattering lengths ($a_s < 0$) of larger magnitude are similar to those for $k_F|a_s| \ll 1$.

B. Spherical (S) GFC

When $\boldsymbol{\lambda} = \frac{\lambda}{\sqrt{3}}(1,1,1)$ a spherical (S) GFC is obtained. Starting from two identical overlapping spheres at $\lambda = 0$, the non-interacting Fermi surfaces of the two helicities continue to be spheres with their centers at the origin of the momentum space for $0 < \lambda < \lambda_T$. Here $\lambda_T = \dfrac{\sqrt{3}}{2^{2/3}} k_F$. When $\lambda \ll \lambda_T$, the chemical potential of the non-interacting system depends on λ as

$$\frac{\mu_{NI}(\lambda)}{E_F} = 1 - \frac{1}{2^{\frac{1}{3}}} \left(\frac{\lambda}{\lambda_T}\right)^2 \quad (\lambda \ll \lambda_T). \tag{34}$$

In this regime, the radius of the + helicity Fermi surface is larger than that of the − helicity Fermi surface. At the FSTT, the − helicity Fermi surface vanishes and ceases to exist for all $\lambda \geq \lambda_T$. After the FSTT, the + helicity Fermi sea is "a sphere with a hole", i. e., a region bounded by two concentric spherical Fermi surfaces. For $\lambda \gg \lambda_T$ the chemical potential of the non-interacting system goes as

$$\frac{\mu_{NI}(\lambda)}{E_F} = \frac{2^{\frac{8}{3}}}{9} \left(\frac{\lambda_T}{\lambda}\right)^4 \quad (\lambda \gg \lambda_T). \tag{35}$$

Consider now the situation when $k_F|a_s| \ll 1$. When $\lambda = 0$, the usual BCS state with properties given by eqn. (32) and eqn. (33) is the ground state. For $\lambda \ll \lambda_T$, μ is very nearly equal to that given by eqn. (34); the gap equation can be solved in this regime to obtain an analytical approximation for the gap as

$$\Delta = \frac{8\mu_{NI}(\lambda)}{\exp\left(\frac{12\mu_{NI}(\lambda)}{6\mu_{NI}(\lambda)+\lambda^2}\right)} \exp\left(-\frac{3\pi\sqrt{\mu_{NI}(\lambda)}}{\sqrt{2}|a_s|(6\mu_{NI}(\lambda)+\lambda^2)}\right). \tag{36}$$

Fig. 4(a) and (b) show, respectively, the numerical solutions of the chemical potential and gap as a function of λ. Fig. 4(a) also shows the non-interacting chemical potential, and the two-body energy $-E_b/2$ (which depends on λ and a_s only). As is evident the chemical potential μ is identical to the non-interacting value $\mu_{NI}(\lambda)$ for $\lambda \ll \lambda_T$. There is also excellent agreement for the gaps obtained from the numerical solution with the analytical approximation given in eqn. (36). When λ approaches λ_T the chemical potential begins to fall below μ_{NI}, and *on further increase of* λ *($\lambda \gtrsim \lambda_T$), the chemical potential tends to that set by the two-body problem.* This clearly signals a crossover from the BCS like state for $\lambda \ll \lambda_T$ to a BEC state where the fermions form tightly bound bosonic pairs which then condense in the zero center of mass momentum state.

Further corroboration of the crossover to the BEC like state with increasing λ can be obtained by a study of the triplet content η_t which is shown in Fig. 4(c). Again, η_t of the non-interacting system monotonically increases

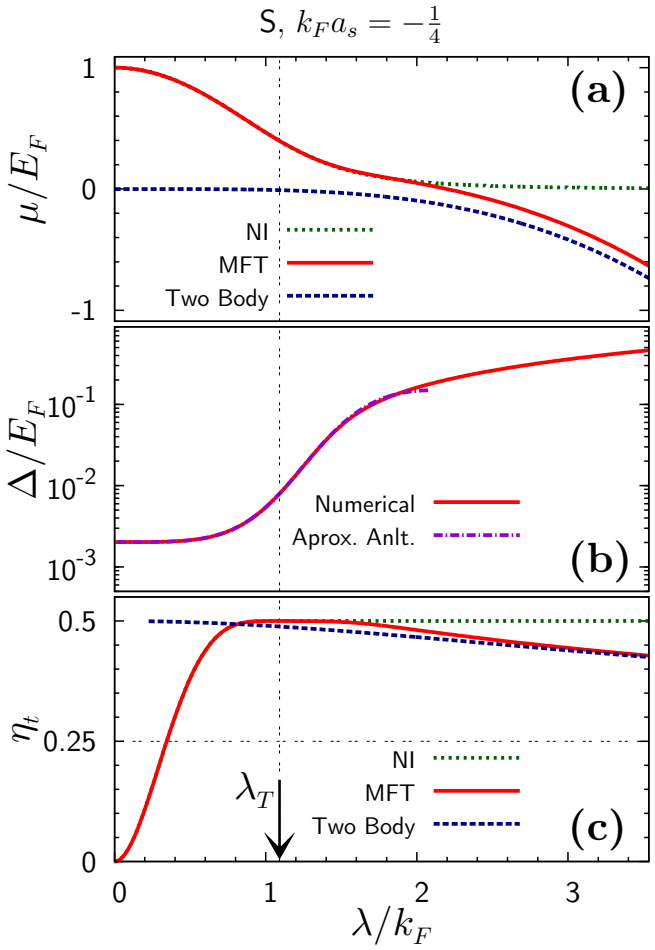

FIG. 4. (Color online) Evolution of the ground state of a collection of interacting fermions ($k_F a_s = -\frac{1}{4}$) with gauge-coupling strength λ for the S GFC. **(a)** Chemical potential obtained from a numerical solution of mean field theory (MFT) is compared with the chemical potential of the non interacting system (NI) and that set by the binding energy of the two-body problem ($-E_b/2$). For $\lambda \lesssim \lambda_T$ the chemical potential is indistinguishable from that of the non-interacting system. For $\lambda \gtrsim \lambda_T$ the chemical potential approaches the two body value indicating a crossover to a BEC. **(b)** Evolution of the numerically obtained mean field energy gap Δ with the gauge-coupling strength λ. The analytical approximation (eqn. (36)) for $\lambda \ll \lambda_T$ is also shown and is indistinguishable from the numerical result. **(c)** The dependence of the triplet content (η_t) of the pair wave function defined in eqn. (29) on the gauge coupling strength. This is compared with the same quantity of the non-interacting system (NI) and with that of the wave function of the two-body bound state. It is seen that the pair wave function evolves to two-body bound-state wave function.

and attains a value of $\frac{1}{2}$ at λ_T. The triplet content of the superfluid pair, as expected, is less than that of the non-interacting system, but has a similar qualitative behavior as the NI case in the regime $\lambda \ll \lambda_T$. The triplet content attains a maximum at a λ close to λ_T and then begins to fall. On further increase of λ, η_t approaches that of the *two-body* bound-state wave function, demonstrating again that the pair wave function tends to the two-body bound-state wave function. We also see that $\lambda = \lambda_T$ marks the crossover point, i. e., the crossover regime is precisely the regime of λ where change in the topology of the non-interacting Fermi sea takes place.

It is particularly interesting to study the BEC state that is attained when $\lambda \to \infty$. The key point as noted in Section II is that the physics of the two-body bound state is determined by the dimensionless parameter λa_s (see Table. I). Therefore, as $\lambda \to \infty$, the parameter $\frac{1}{\lambda a_s} \to 0$. Thus the state that is obtained is same as that obtained for the two-body bound state with a resonant scattering length *in the presence of the gauge field ($\lambda > 0$)* (Table. I)! Therefore *the properties of the BEC for $\lambda \to \infty$ are completely determined by $\boldsymbol{\lambda}$, independent of the scattering length (as long as it is non vanishing, see Fig. 5)*, i. e., the system is a collection of bosons whose properties are determined solely by the Rashba interaction. Hence we call this tightly bound bosonic state of two fermions as "rashbon". Rashbon is a bound state of two fermions in a Rashba gauge field ($\lambda > 0$) at resonant scattering length ($\frac{1}{a_s} = 0$).

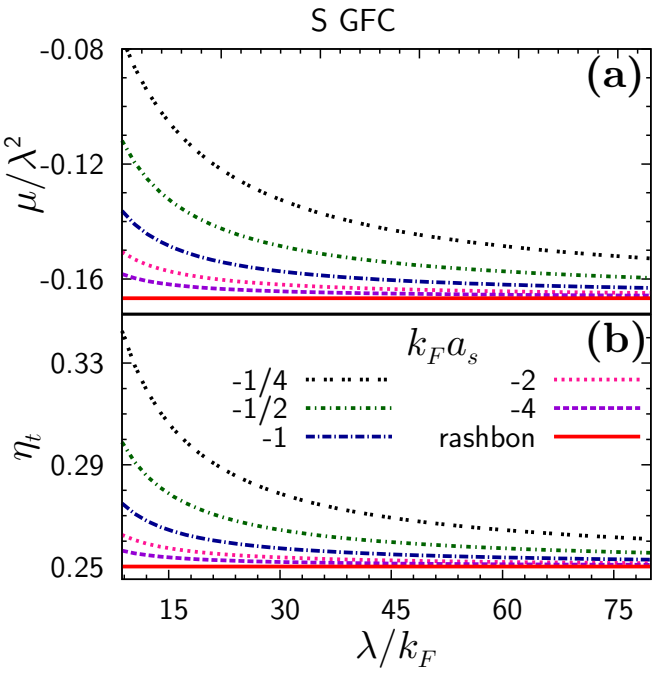

FIG. 5. (Color online) Dependence of chemical potential (μ) and triplet content (η_t) on gauge-coupling strength λ (S GFC) in the $\lambda \gg \lambda_T$ regime, for various scattering lengths a_s. **(a)** Chemical potential, for all scattering lengths, asymptotically attains the value set by the rashbon energy (see Table I) as $\lambda/k_F \to \infty$. **(b)** Triplet content also attains the rashbon value independent of the scattering length.

C. Extreme oblate (EO) GFC

The evolution of the non interacting Fermi surfaces for this GFC ($\boldsymbol{\lambda} = \frac{\lambda}{\sqrt{2}}(1,1,0)$ is shown in fig. 2. The non-interacting chemical potential in the regime $\lambda \ll \lambda_T$ is

$$\frac{\mu_{NI}(\lambda)}{E_F} = 1 - \left(\frac{4}{3\pi}\right)^{\frac{2}{3}} \left(\frac{\lambda}{\lambda_T}\right)^2 \quad (\lambda \ll \lambda_T) \tag{37}$$

and that in the regime $\lambda \gg \lambda_T$ is

$$\frac{\mu_{NI}(\lambda)}{E_F} = \left(\frac{4}{3\pi}\right)^{\frac{2}{3}} \frac{\lambda_T}{\lambda} \quad (\lambda \gg \lambda_T). \tag{38}$$

To illustrate that the qualitative nature of the crossover is unaltered by the size of the scattering length, we study this GFC at the resonant scattering length $1/k_F a_s = 0$. The results are shown in fig. 6. These results clearly illustrate a crossover from the resonant superfluid (in the absence of the gauge field) to a rashbon BEC. The crossover obtained at resonance is "smoother" than that for $k_F|a_s| \ll 1$.

It is also interesting to discuss the dispersion of the Bogoliubov quasiparticles with particular focus on the "topology transition" of their dispersion (which takes place for all GFCs). The term "transition" is used in the same sense as that in the non-interacting case (FSTT) and does not, again, indicate the emergence or vanishing of a new order parameter. At the transition, the topology of the constant-energy surfaces of the quasiparticles in $\boldsymbol{k}$ space changes. This change in topology is also accompanied by low energy excitations of only the + helicity. To this end, we introduce the gauge-coupling strength λ_B at which the transition occurs. For a non-positive scattering length ($a_s < 0$), the gauge-coupling strength at which the chemical potential $\mu(\lambda)$ equals that of the non-interacting system at the FSTT defines λ_B, i. e.,

$$\mu(\lambda_B) = \mu_{NI}(\lambda_T) \tag{39}$$

Note that λ_B, in general, depends on the scattering length a_s with $\lambda_B \approx \lambda_T$ when $k_F|a_s| \ll 1$. Fig. 7 shows the evolution of the quasiparticle dispersion with increasing gauge-coupling strength. When $\lambda < \lambda_B$, we see that there are

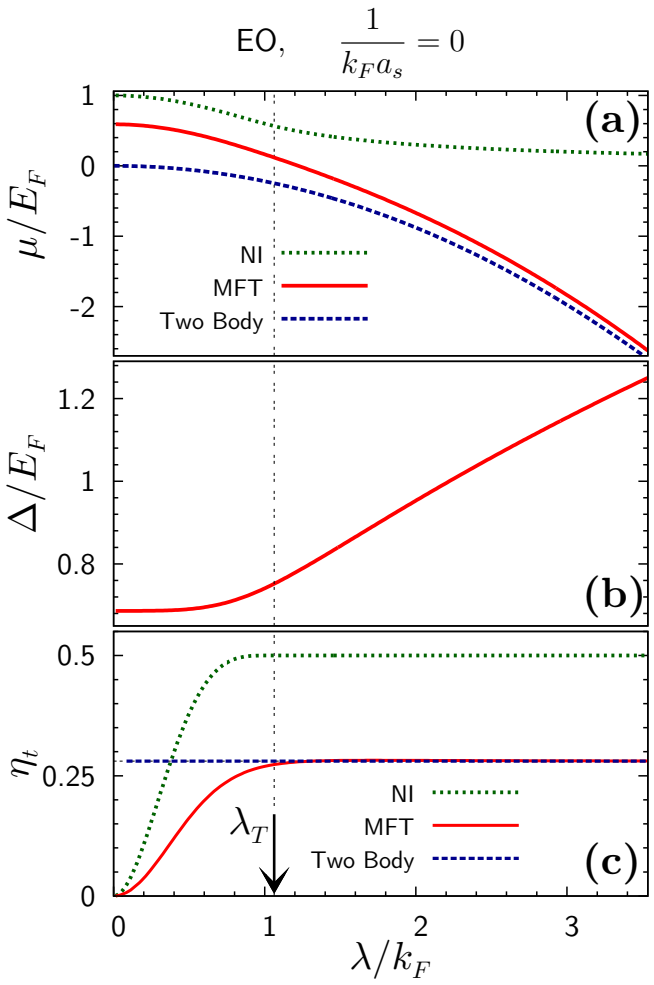

FIG. 6. (Color online) Evolution of the ground state of a collection of resonantly interacting fermions ($\frac{1}{k_F a_s} = 0$) with gauge-coupling strength λ for the EO GFC. **(a)** Chemical potential obtained from a numerical solution of mean field theory (MFT) is compared with the chemical potential of the non interacting system (NI) and that set by the binding energy of the two-body problem ($-E_b/2$). For $\lambda \lesssim \lambda_T$ the chemical potential is changed significantly from the NI value due to large interactions. For $\lambda \gtrsim \lambda_T$ the chemical potential approaches that set by the rashbon value. There is a crossover from a resonant superfluid (at $\lambda = 0$) to a rashbon BEC as $\lambda/k_F \to \infty$. **(b)** Evolution of the numerically obtained mean field energy gap Δ with the gauge-coupling strength λ. **(c)** The dependence of the triplet content (η_t) of the pair wave function defined in eqn. (29) on the gauge-coupling strength. The triplet content of the pair wave function evolves to that of the rashbon.

low lying quasiparticle excitations of *both* helicity. At $\lambda = \lambda_B$, the low lying $-$ helicity excitation appears at $\boldsymbol{k} = 0$, and for $\lambda > \lambda_B$, the there are no low-lying excitations corresponding to $-$ helicity. It is evident from Fig. 7 that there is a transition in the topology of the dispersion of the Bogoliubov quasiparticles at λ_B. Clearly, this can be traced to the FSTT, and indeed for $k_F|a_s| \ll 1$, this transition in the quasi particle spectrum very nearly coincides with FSTT.

V. SUMMARY AND DISCUSSION

Here we summarize the work carried out and the new results of this paper:

1. We have studied, using mean field theory, the evolution of the *many body ground state wave function* of a finite density of interacting spin-$\frac{1}{2}$ fermions in a non-Abelian gauge field with increasing gauge coupling.

2. We show that a non-Abelian gauge field, which produces a spin-orbit coupling of the Rashba type, engenders a crossover from a BCS ground state to a BEC ground state of bosons even for a weak attractive interaction (small negative scattering length).

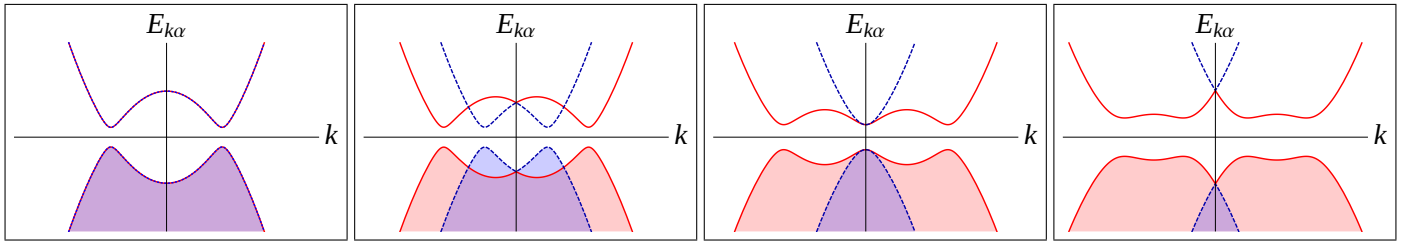

(a) $\lambda = 0$ **(b)** $0 < \lambda < \lambda_B$ **(c)** $\lambda = \lambda_B$ **(d)** $\lambda > \lambda_B$

FIG. 7. (Color online) Evolution of the Bogoliubov quasiparticle dispersion with gauge coupling λ. Solid lines (red) correspond to + helicity quasiparticles, while the dashed (blue) ones are for − helicity. The shading represents occupied states. The horizontal lines mark the chemical potential. The gauge coupling λ_B is that at which the chemical potential μ equals that of the non-interacting system at FSTT ($\mu(\lambda_B) = \mu_{NI}(\lambda_T)$). **(a)** The standard BCS dispersion in the absence of the gauge field. **(b)** The gap of excitation of quasiparticles for both helicities are equal. **(c)** Transition point in the topology of the Bogoliubov dispersion **(d)** The negative helicity quasiparticles have a higher gap; low lying quasiparticles are only of + helicity. All the dispersions shown are for the EO GFC with $k_F a_s = -1$ for excitation momenta along $(1, 0, 0)$. The critical gauge coupling in this case is $\lambda_B \approx 1.03\, k_F$.

3. For large gauge couplings, the BEC that forms is a condensate of bosons whose properties are determined entirely by the Rashba gauge field (and not by any other scale in the system). These bosons have many features different from bound bosonic pair in free vacuum (no gauge field) and we have called them "rashbons" to bring out this point clearly.

4. We demonstrate that in the absence of interactions the Fermi surface of the system undergoes a topology change at a critical value of gauge coupling. We call this the Fermi surface topology transition (this is *not* a phase transition with an associated order parameter) since the genus of the Fermi surface changes at the critical gauge coupling. We show that for weak attractive interactions, the regime of the crossover from the BCS to BEC occurs around the critical gauge coupling that causes the Fermi surface topology transition.

5. These results make a novel suggestion of obtaining a BCS-BEC crossover through a new route i. e., by tuning the spin-orbit interaction.

We conclude the paper with further discussion of our results. On the BCS side ($k_F|a_s| \ll 1$ and $\lambda \ll \lambda_T$), the transition temperature will be determined by the zero temperature gap which we have calculated in this paper. On the rashbon BEC side, the transition temperature will be determined by the mass of these emergent bosons[25] which will be renormalized by the gauge field (and *not* twice the bare fermion mass).

As noted earlier, the rashbon is a bound state of two fermions in a Rashba gauge field ($\lambda > 0$) when the s-wave scattering length is infinity, i.e., at resonance. This two-fermion bound state exists for *all* GFCs except the EP GFC and has a spin structure determined by $\hat{\boldsymbol{\lambda}}$ of the GFC (see the "resonance" column of Table. I). As is evident this state is not rotationally symmetric – it is an "anisotropic particle" that emerges. It is also interesting to contrast the rashbon state obtained in a Rashba gauge field ($\lambda > 0$) with the two-body quasi-bound state obtained in free vacuum ($\lambda = 0$) at resonance. In the latter case, the binding energy is zero, and the state is scale free with a singlet spin structure. This is to be contrasted with the rashbon state whose binding energy is λ^2 times a dimensionless number that depends on $\hat{\boldsymbol{\lambda}}$. Indeed, the rashbon state is not scale free – the wave function in the relative coordinate of the two fermions dies exponentially with a scale λ^{-1} as noted in reference [20].

For a generic GFC, it is known that the critical scattering length a_{sc} required to induce a bound state is negative and finite[20] and is given by $a_{sc} = \frac{\mathcal{F}(\hat{\boldsymbol{\lambda}})}{\lambda}$ where $\mathcal{F}$ is a dimensionless function. For a *given* $a_s < 0$, this corresponds to a critical gauge-coupling strength $\lambda_c = \left|\frac{\mathcal{F}(\hat{\boldsymbol{\lambda}})}{a_s}\right|$. The crossover with increasing λ is then governed by the relative magnitudes of λ_T and λ_c. If $\lambda_c \lesssim \lambda_T$, the crossover regime coincides with the regime of the FSTT. On the other hand if $\lambda_c \gg \lambda_T$, the crossover regime is centered around $\lambda \approx \lambda_c$. In any case, for $\lambda \gg \max(\lambda_T, \lambda_c)$ the ground state will be a condensate of rashbons determined by the GFC in question. It is evident that except for the EP GFC, every other GFC will support a BCS-rashbon BEC crossover.

We now discuss the situation with a small positive scattering length with $k_F a_s \ll 1$. In absence of a gauge field, the ground state is a BEC of bosonic pairs of fermions with mass (nearly) twice that of the fermion mass. In the presence of the gauge field, this BEC will evolve to the rashbon BEC as $\lambda \to \infty$, i.e, there is a BEC-rashbon BEC crossover.

It is also interesting to discuss the issue of gauge invariance in the context of synthetic gauge fields. It must be noted that the experimental synthetic gauge fields[1–3] make a particular gauge choice, i. e., they are an implementation of a particular gauge. Any other gauge field that is "gauge related" will produce the same physical results. In our case all gauge fields that are related by a SU(2) gauge transformation to the ones that are considered here will produce same physical results as found here.

The authors are not aware of any experimental realization of synthetic gauge fields in fermionic systems. The natural question that arises is if the parameter regime of $\lambda \gtrsim \lambda_T$ with a high-symmetry GFC can be realized in experiments. We do hope that our paper provides the motivation for this direction of experimental research.

Acknowledgement

JV acknowledges support from CSIR, India via a JRF grant. SZ is supported by NSF DMR-0907366 and DARPA Nos. W911NF-07-1-0464 . VBS is grateful to DST, India (Ramanujan grant) and DAE, India (SRC grant) for generous support. We are grateful to Tin-Lun (Jason) Ho for discussions.

---

* jayantha@physics.iisc.ernet.in
† shizhong.zhang@gmail.com
‡ shenoy@physics.iisc.ernet.in

[1] Y.-J. Lin, R. L. Compton, A. R. Perry, W. D. Phillips, J. V. Porto, and I. B. Spielman, Phys. Rev. Lett. **102**, 130401 (2009).
[2] Y.-J. Lin, R. L. Compton, K. Jimenez-Garcia, J. V. Porto, and I. B. Spielman, Nature **462**, 628 (2009).
[3] Y.-J. Lin, K. Jimenez-Garcia, and I. B. Spielman, Nature **471**, 83 (2011).
[4] K. Maeda, G. Baym, and T. Hatsuda, Phys. Rev. Lett. **103**, 085301 (2009).
[5] D. Jaksch and P. Zoller, New Journal of Physics **5**, 56 (2003).
[6] K. Osterloh, M. Baig, L. Santos, P. Zoller, and M. Lewenstein, Phys. Rev. Lett. **95**, 010403 (2005).
[7] J. Ruseckas, G. Juzeliūnas, P. Öhberg, and M. Fleischhauer, Phys. Rev. Lett. **95**, 010404 (2005).
[8] F. Gerbier and J. Dalibard, New Journal of Physics **12**, 033007 (2010).
[9] See commentary on reference [3] by T.-L. Ho at http://www.condmatjournalclub.org.
[10] W. Ketterle and M. W. Zwierlein, "Making, probing and understanding ultracold Fermi gases," (2008), arXiv:0801.2500 [cond-mat].
[11] I. Bloch, J. Dalibard, and W. Zwerger, Rev. Mod. Phys. **80**, 885 (2008).
[12] S. Giorgini, L. P. Pitaevskii, and S. Stringari, Rev. Mod. Phys. **80**, 1215 (2008).
[13] D. M. Eagles, Phys. Rev. **186**, 456 (1969).
[14] A. J. Leggett, in *Modern Trends in the Theory of Condensed Matter*, edited by A. Pekalski and R. Przystawa (Springer-Verlag, Berlin, 1980).
[15] A. J. Leggett, *Quantum Liquids: Bose Condensation and Cooper Pairing in Condensed-Matter Systems* (Oxford University Press, 2006).
[16] P. Noziéres and S. Schmitt-Rink, Journal of Low Temperature Physics **59**, 195 (1985).
[17] M. Randeria, in *Bose-Einstein Condensation*, edited by A. Griffin, D. Snoke, and S. Stringari (Cambridge University Press, 1995) Chap. 15.
[18] T.-L. Ho and S. Zhang, "Bose-Einstein Condensates in Non-abelian Gauge Fields," (2010), arXiv:1007.0650 [cond-mat.quant-gas].
[19] C. Wang, C. Gao, C.-M. Jian, and H. Zhai, Phys. Rev. Lett. **105**, 160403 (2010).
[20] J. P. Vyasanakere and V. B. Shenoy, Phys. Rev. B **83**, 094515 (2011).
[21] E. Braaten, M. Kusunoki, and D. Zhang, Annals of Physics **323**, 1770 (2008).
[22] It is to be noted that the result for the EO case presented in [20] has a minor error of a factor of 2. The correct results are quoted here; see also Section III B of e-print arXiv:1101.0411v2.
[23] Throughout the paper, the chemical potential is referred to the bottom of the + helicity band.
[24] R. B. Diener, R. Sensarma, and M. Randeria, Phys. Rev. A **77**, 023626 (2008).
[25] J. P. Vyasanakere and V. B. Shenoy, (2011), under preparation.